THE
IRISH ASTRONOMICAL
JOURNAL

Vol. 8 December 1968 No. 8

STAR CHAINS AROUND ETA CARINAE

H. H. R. Grossie and E. J. Öpik

Abstract

On an ADH red sensitive plate without filter, 69 star chains, mostly ring-shaped and containing 10-30 members each, on a scale from 0′.6 to 4′.5, have been listed. The total area searched contains about 400,000 stars down to 20th magnitude. Probability criteria, specially developed and applied to these chains, indicate that for purely geometrical reasons about 60% of them must be non-random real groupings of a high statistical level of confidence, and many of the remainder may be, too, on account of the brightness of their members. Further more detailed research is planned.

Experiments with particles suspended in a liquid, or with falling droplets, cannot claim to have fulfilled the conditions of randomness especially because of microturbulence and vorticity of the media. Purportedly "random" chains so produced are not random at all.

1. *Introduction*

An inspection of ADH plates of the η Carinae region leaves one with an inescapable impression that the stellar distribution there is far from being random. Apart from the obvious large-scale irregularities, apparently caused by absorbing dustclouds (*cf. Ref.* 1, Plate V), there are small groupings such as star chains, chiefly of the closed or open ring type, unusual looking groups of brighter stars of similar magnitude, and some typical dark globules. The region seems to be particularly suitable for the study of the much-disputed problem of star chains. Are these groupings real, either caused by absorbing globules leaving stars visible on their periphery, or by true chain-like stellar associations, young stars just born in a shell or along wisps of diffuse interstellar matter ? Or are they purely chance configurations, picked out from a great number of random groupings ?

With these questions in mind, ADH plate No. 1076 (emulsion 103aE red sensitive without filter, corresponding to a wide band of "panchromatic" light) was examined and measured by one of us (G) (unprejudiced by previous experience) for small unusual looking groupings. The emphasis was on stellar groups, not on dark absorbing globules although some of them are also noted.

The theoretical treatment and discussion is entirely the responsibility of the other co-author (Ö).

Particulars of the ADH telescope have been published by Lindsay (*Ref.* 2). The area on the circular plate covers 18.2 square degrees, but the effective area searched equals 30,000 mm² or 10.8 square degrees; the actual scale of this exposure was 68″.09 per mm. The middle of the plate is at $\alpha = 10^h\ 43^m$, $\delta = -59°10'$ (1875.0), galactic longitude 288° (II), latitude 0°.

2. *Catalogue of the Unusual Groupings*

The groupings were picked out by subjective impression. This involves ignoring background stars fainter than a certain limiting magnitude, characteristic of each grouping. The "voids" around the chains are thus relative to this subjective limit, while fainter stars may always be present.

Table 1 lists the groupings. The search was made on a microscope, and the objects so noted were measured on an iris diaphragm photometer. The field covered by the latter was somewhat narrower than that of the microscope, so that some objects of the searching list were not measured; these and some others account for the gaps in the numbering. The first column gives the identification number which thus is not meant to represent a continuous sequence. Only those objects within the limited region (10.8 sq. deg.) for which measurements were made are listed. The second and third columns contain right ascension and declination of the middle point of the configuration for 1875.0. Column 4 gives the total number, n, of stars registered in the grouping (chain). Column 5 states the total estimated area, s, enclosing the grouping, as limited by an elliptical outline, and which is supposed to contain only those n stars registered in the grouping brighter than an unspecified subjective limiting magnitude. The sixth and seventh columns show n_r, the number of stars belonging to the chain, and s_r, the area enclosed by elliptical or oval contours containing n_r; usually $n_r = n$, sometimes one, two or three stars considered stray had to be excluded, in which case $n_r < n$. The eighth column gives s_i, that area of the relative void inside the chain (ring). When $n_r = n$, another relative void outside the chain has an area of s-s_r-s_i. The areas are given in mm²; on the scale of the plate, 1mm² = 1.29 square minutes of arc. Column 9 gives w, the difference in surface brightness of the field background between the area inside and outside the chainlike closed or semi-closed grouping, in units of the photometric wedge (unit about 0.07 mag), derived as the average of a number of points where no obvious star images were seen; positive w means that the "interior" is brighter, negative w—that it is darker than the "exterior", the latter case being conspicuous in the globules; the spread in the individual w-values shows a probable deviation of ± 1.0 units and is chiefly caused by random fluctuations of the background of invisible stars.

Columns 10, 11 and 12 contain "conventional magnitudes" as measured on the iris diaphragm photometer: m_o, the median or 50 per cent divide of the group; m_f, the faintest magnitude in the group; and m_b, the "background

Table 1

Star Groupings in the Field of Eta Carinae

Abbreviations: Rg, *ring*; Neb, *nebulosity*; Gl, *dark globule*; Ch. *star chain*; Sp, *spiral;* Dis, *distorted*; Db, *double*; App, *appendage*; Cl, *cluster*; Op, *open*; Br, *bright*. In 13th column, $1.8^{-16} = 1.8 \times 10^{-16}$, etc.

(1) No.	(2) α 10^h+	(3) $-\delta$ ° ′	(4) n	(5) s	(6) n_r	(7) s_r	(8) s_i	(9) w	(10) m_o	(11) m_f	(12) m_b	(13) E	(14) Remarks
13	$32^m.9$	60 46	18	0.82	18	0.43	0.39	+0.4	18.0	19.9	20.1	0.82	Rg, Neb
14	31.5	60 27	19	5.7	18	0.31	3.8	−5.7	faint		19.8	1.8^{-16}	Gl, Ch
16	36.4	60 53	16	0.66	16	0.26	0.33	+1.8	17.8	18.8	20.0	0.048	Rg
17	36.5	60 49	13	0.43	13	0.16	0.25	+3.7	17.5	19.4	19.8	0.52	Op Rg
18	33.2	60 27	16	0.75	16	0.23	0.39	+1.5	18.0	19.3	19.7	6.0^{-4}	Rg
19	35.7	60 41	14	0.55	12	0.17	0.20	+5.8	16.9	18.7	20.0	22.	Rg
20	38.0	60 55	42	5.5	39	1.2	3.1	−1.0	16.0	18.7	20.2	5.6^{-18}	Sp Ch
21	39.2	61 05	34	3.1	34	1.06	1.20	−1.1	17.0	19.5	20.2	4.1^{-12}	Dis Rg
22	38.6	61 01	15	1.64	15	0.55	0.83	+0.6	16.7	18.3	20.2	0.0041	Rg
23	24.3	59 08	8	0.22	8	0.09	0.12	0.0	18.5	19.0	20.2	320.	Rg
24	32.2	59 54	12	0.38	11	0.08	0.14	+8.9	17.0	18.5	19.7	10.	Op Rg
25	34.7	60 12	12	0.69	11	0.23	0.31	0.0	17.5	18.2	19.8	14.	Rg
26	37.6	60 38	18	0.86	16	0.43	0.37	−0.1	17.6	18.8	19.9	5.6	Rg
27	32.8	59 54	30	2.5	30	1.34	0.97	−0.1	16.4	19.0	19.4	2.6^{-4}	Sp Ch
28	34.6	60 02	35	1.9	35	0.56	1.02	−1.5	16.6	18.3	19.6	1.2^{-14}	Db Rg
29	41.1	60 40	14	0.78	14	0.24	0.44	−1.1	18.1	19.6	20.1	0.0080	Rg
30	35.8	59 56	17	1.4	15	0.36	0.58	0.0	16.5	18.2	19.2	0.055	Rg
31	33.7	59 33	6	…	…	…	7.2	−7.1	…	…	19.5	…	Gl, Rg
32	34.7	59 28	14	1.4	14	0.39	0.65	+0.8	16.2	17.1	19.2	0.0011	Op Rg
33	37.8	59 27	8	0.33	8	0.11	0.12	+2.4	(13.3	14.8)	17.8	4.1	Rg, Neb
35	41.0	59 41	8	0.36	8	0.28	0.08	+2.1	16.4	17.2	19.0	33000.	Op Rg
36	38.4	59 11	13	0.78	13	0.32	0.27	−3.0	(11.5	13.0)	16.7	1.1	Rg, App
37	36.1	58 57	18	4.3	18	1.28	2.17	+1.1	(13.7	15.5)	17.2	7.1^{-6}	Sp Ch
38	32.9	58 41	16	1.20	16	0.37	0.53	+1.2	16.5	18.9	19.8	5.0^{-4}	Rg, App
39	43.9	59 47	11	0.93	11	0.36	0.25	−0.3	15.3	17.1	18.9	3.0	Op Rg
42	37.6	58 18	17	1.62	17	0.36	0.58	+2.0	(17.0	17.6)	17.8	4.3^{-7}	Rg, Neb
43	38.6	58 12	17	1.86	17	0.69	0.86	−0.2	(14.1	15.7)	17.8	0.0024	Rg, Neb
45	37.8	57 53	44	2.80	44	1.00	1.22	+0.2	16.9	18.7	19.4	7.7^{-15}	Db Ch
46	44.1	58 41	12	1.20	12	0.39	0.60	−1.4	14.4	17.5	18.9	0.10	Br Rg
47	35.4	57 31	5	0.31	5	0.15	0.16	−0.3	13.0	14.6	19.9	7800.	Br Ch
49	52.5	59 04	12	0.56	12	0.33	…	+3.9	15.1	16.8	19.4	290.	Cl
50	53.0	58 56	11	0.44	11	0.22	0.14	+0.6	15.0	16.9	19.6	100.	Br Rg
51	51.2	58 47	10	1.57	10	0.43	0.78	+0.2	14.7	17.4	19.7	0.14	Op Rg
52	50.1	58 38	16	2.35	14	0.63	0.89	+1.5	15.4	18.2	19.8	0.27	Op Rg
53	41.8	57 34	15	1.54	13	0.59	0.44	−0.4	17.0	18.2	20.0	3.0	Rg, App

Table 1. *Continued*

(1) No.	(2) α	(3) $-\delta$	(4) n	(5) s	(6) n_r	(7) s_r	(8) s_i	(9) w	(10) m_o	(11) m_f	(12) m_b	(13) E	(14) Remarks
	10^h+	° ′											
54	$45^m.5$	57 50	16	2.0	16	0.79	0.58	—0.4	16.8	18.7	19.8	0.016	Rg, App
55	49.8	58 12	9	0.56	8	0.12	0.30	—2.7	14.8	16.6	19.5	9.5	Rg
56	46.6	57 47	10	0.41	9	0.18	0.23	+1.9	16.0	18.4	19.6	130	Rg
57	44.4	57 22	5	0.24	5	0.07	...	—1.0	14.9	15.0	19.8	88.	Br Ch
58	49.1	57 56	14	1.6	14	0.45	...	+0.4	15.6	17.9	19.7	0.028	Ch
59	41.6	56 48	14	1.25	13	0.28	0.74	—4.1	17.5	18.7	19.8	0.0045	Ch
60	50.0	57 53	18	4.5	18	2.0	2.5	—1.4	15.6	18.6	20.2	0.0087	Op Rg
61	44.4	57 02	8	0.42	8	0.13	0.12	+1.1	16.4	17.8	20.1	18.	Op Rg
62	43.9	56 55	17	6.4	17	3.4	2.9	—0.2	15.2	18.6	20.1	0.29	Rg
63	43.3	57 13	14	1.62	14	0.41	0.87	—0.9	17.3	19.1	20.1	2.4^{-4}	Rg
64	52.8	57 44	6	2.0	6	0.23	0.94	...	16.2	17.1	20.0	0.10	Ch in Gl
65	50.6	57 53	18	...	...	...	...	—0.6	...	...	20.0	...	Gl
66	53.0	58 07	24	12.8	21	4.0	6.2	—2.6	16.7	19.6	20.1	2.5^{-5}	Rg
69	35.5	60 21	6	0.42	6	0.14	0.20	+0.8	16.6	17.0	20.2	310.	Rg
72	30.1	60 12	19	2.8	19	1.54	1.10	+0.8	17.2	18.6	19.8	0.37	Rg
73	26.3	59 33	27	...	...	...	...	—0.2	...	...	20.1	...	Gl
74	39.0	60 59	23	1.76	23	0.51	0.65	—0.7	17.3	18.9	20.2	2.1^{-8}	Rg, App
75	39.9	60 56	11	1.29	11	0.29	0.58	—1.4	16.3	18.2	20.2	0.0052	Op Rg
76	39.5	60 53	10	0.24	10	0.12	0.08	+5.0	17.7	19.1	20.1	360	Rg
77	28.0	59 37	10	0.56	10	0.18	0.31	—0.6	17.5	17.8	20.0	1.9	Op Rg
78	34.3	60 09	16	0.70	16	0.34	0.20	0.0	16.2	17.9	19.6	1.2	Op Rg
79	38.1	60 37	...	...	...	...	...	—1.4	...	...	19.8	...	Gl
80	38.7	61 08	19	1.8	19	0.94	0.36	—1.4	17.0	18.0	19.9	0.22	Rg
81	41.0	61 07	13	1.25	13	0.62	...	+3.7	16.3	17.7	19.7	7.9	Ch
82	43.3	60 58	24	2.86	24	1.25	0.77	+2.2	16.6	18.1	19.9	7.1^{-5}	Rg, App
83	44.8	60 31	12	0.95	12	0.66	0.41	+1.0	17.0	18.1	19.5	1200.	Rg
84	45.8	60 14	11	2.1	11	0.69	1.14	+0.8	16.0	16.7	19.4	0.21	Op Rg
85	49.0	59 36	12	1.98	12	1.21	0.70	+1.1	15.2	17.0	19.0	130.	Op Rg
87	50.4	59 10	10	1.5	...	...	...	+2.8	16.0	18.1	19.0	...	Cl
88	51.1	59 06	27	...	...	...	...	—1.3	...	...	19.2	...	Gl, Ch
90	53.0	58 40	12	1.02	12	0.67	0.33	+0.7	16.2	17.2	19.3	580.	Rg
91	55.4	58 33	14	2.64	12	0.53	1.18	+1.3	15.6	17.0	19.2	0.033	Rg
92	55.3	58 59	11	1.13	10	0.26	0.76	+1.7	16.0	17.1	19.0	0.10	Rg
95	41.9	61 22	18	3.2	18	0.87	1.19	+0.4	16.4	18.0	19.9	1.9^{-6}	Rg, App
96	45.8	60 43	17	2.2	17	0.32	1.02	+0.2	17.0	18.7	19.6	2.6^{-10}	Sp Ch
97	48.4	60 22	22	2.2	22	1.00	0.98	+0.6	16.5	17.8	19.4	0.012	Cl, Ch
98	53.4	59 46	8	0.27	8	0.12	0.14	+0.6	16.7	17.8	19.2	510.	Op Rg
99	58.3	59 06	7	0.31	7	0.10	0.14	—0.2	17.5	18.4	19.4	110.	Op Rg
101	47.6	57 21	15	1.91	15	0.75	1.16	0.0	16.5	18.3	19.4	0.038	Rg
102	40.6	58 03	9	0.78	8	0.24	0.40	—1.0	16.3	17.7	19.0	55.	Op Rg

magnitude " purportedly showing the background intensity on a scale so chosen that it corresponds to iris reading (linearly extrapolated) on the background without visible stellar images. The magnitude scale for the plate as a whole was adjusted to the star counts of Seares and van Rhijn (*Ref.* 3), and, when $m_b > 19$, the magnitudes are more or less reliable. However, no corrections for background were made, so that the " magnitudes " correspond to a kind of combination of star and background and, when the latter was strong as in the nebula, the stellar brightnesses as listed in the table are greatly over-estimated; these cases are enclosed in brackets.

In the thirteenth column, *E*, the cumulative random expectation of the grouping is given, calculated according to a conventional rule as explained in Sections 5 and 6. It is supposed to represent the expected number of random groupings, of a probability equal or smaller than that of the configuration listed, for a search in the total area of 30,000 mm² covered.

The last, fourteenth column specifies the character of the grouping in the code explained at the top of the table.

Figs. 1 - 3 are charts of the groupings made to scale. The positions are in *X* and *Y* coordinates, in mm, as measured on the photometer. Figs. 1, 2, and 3 represent positions and relative magnitudes of the stars whose magnitudes measured with the iris-diaphragm photometer are recorded separately in Figs. 1a, 2a, and 3a facing the charts, on which also the assumed area contours of the groupings are drawn (those defining s_r and s_i). In such a manner the configurations of the charts can be studied on Figs. 1-3 without interference from the numerals showing the magnitudes. As already mentioned, the magnitude scale was derived from star counts and may contain a considerable error of zero point strongly influenced by the background; in the context of this study the error is irrelevant, the magnitudes being used solely as an intermediary for estimating average star densities per unit area i.e. for expressing the results of star counts from which they were themselves derived.

In the charts, the measured coordinates *X*, *Y* are given directly without transforming them into spherical coordinates. The transformation to α, δ (1875.0) can be achieved with the aid of equations (1) - (4) as follows.

Standard rectangular astrometric coordinates, ξ and η (in seconds of arc) are determined from

$$\xi = A\ (X—430) + B\ (Y—130) + C, \qquad (1)$$

$$\eta = B\ (X—430) — A\ (Y—130) + D, \qquad (2)$$

where $A = 50''.96$, $B = 45''.16$, $C = —5'', \pm 13''$, $D = —154'' \pm 13''$. These are related to right ascension and declination through

$$(\alpha — \alpha_0)'' = \xi'' \sec\ (\delta_0 + \eta) \qquad (3)$$

$$(\delta — \delta_0)'' = \eta'' — [(\alpha — \alpha_0)'']^2 \sin 2\ \delta_0/825000, \qquad (4)$$

where southern declination is conveniently treated as positive, $\delta_0 = +59°10'$ (south), $\alpha_0 = 10^h43^m0^s$ (1875.0). The coefficients of eqs. (1) and (2) were determined by standard astrometric procedure, using positions of reference stars as listed in Table 2.

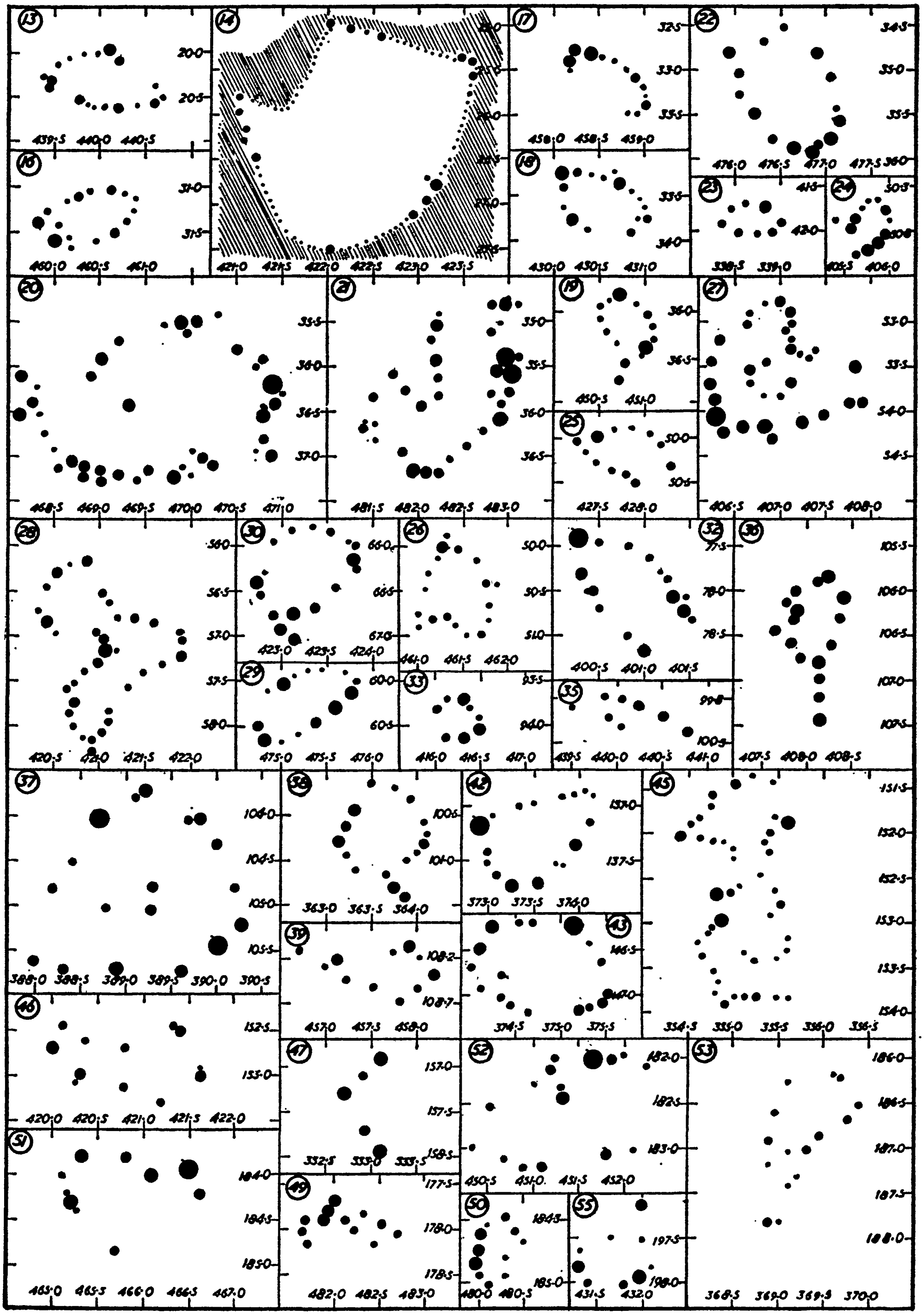

Fig. 1

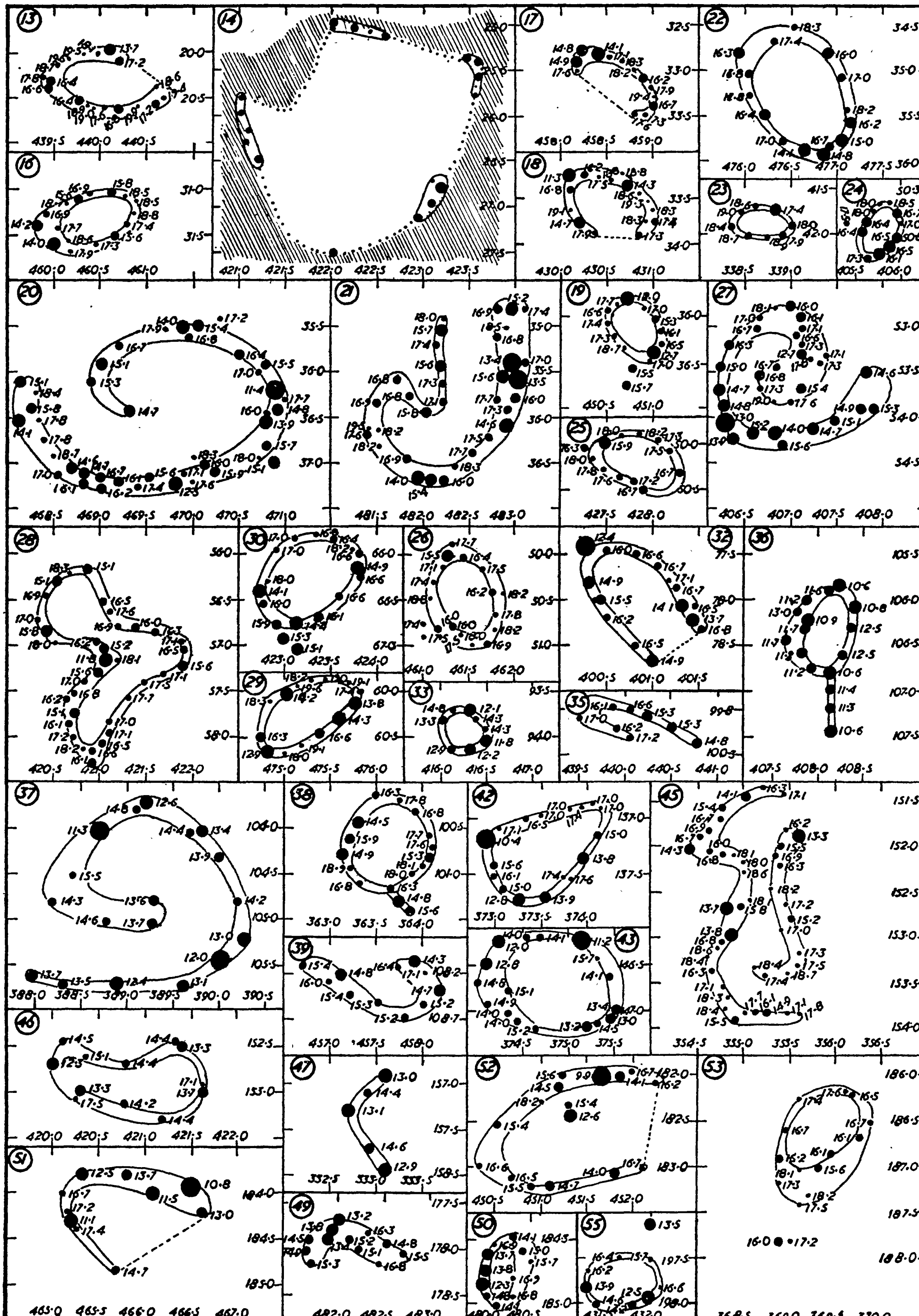

Fig. 1a

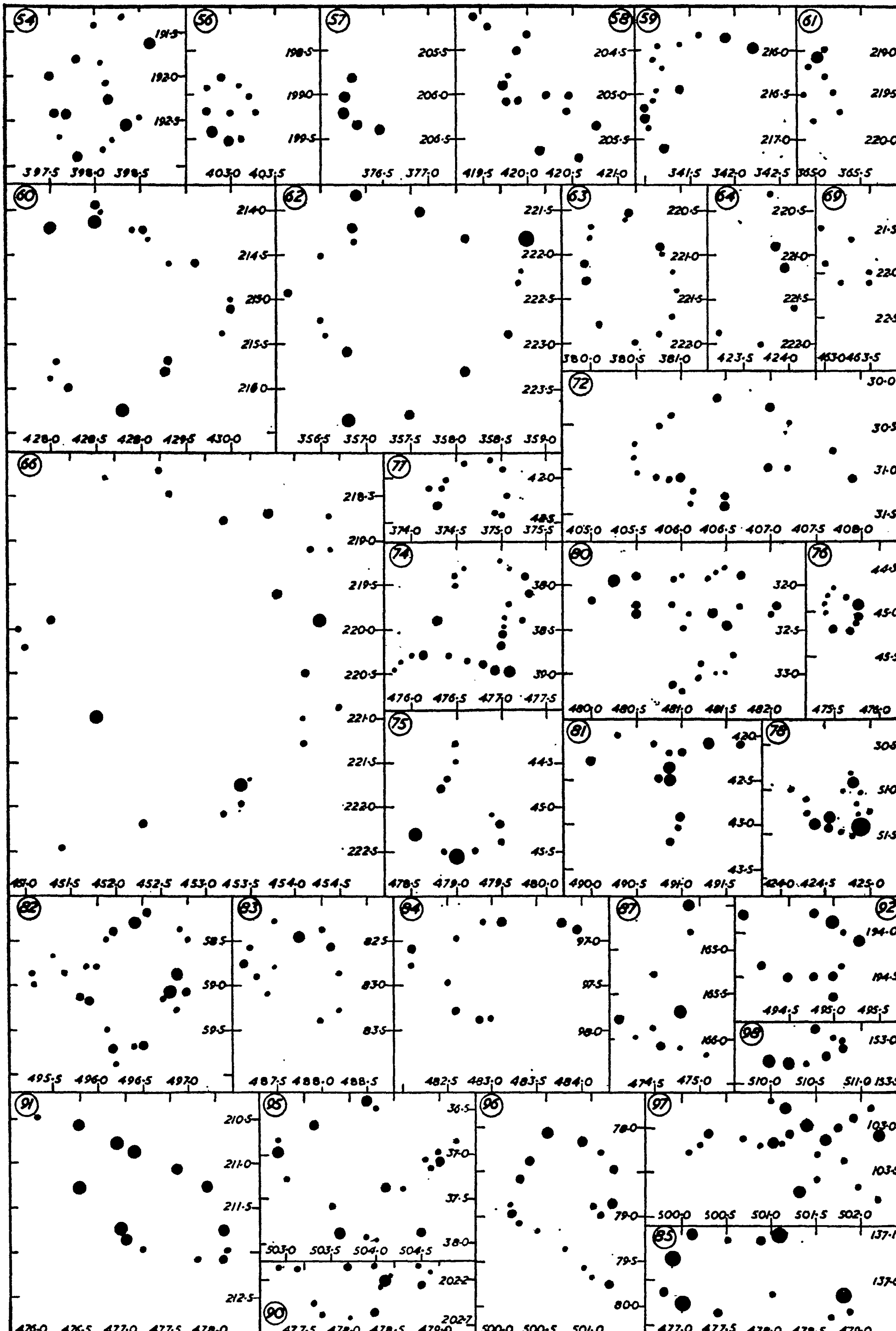
54
56
57
58
59
61
60
62
63
64
69
72
66
77
74
80
76
75
81
78
82
83
84
87
92
98
91
95
96
97
85
90

Fig. 2

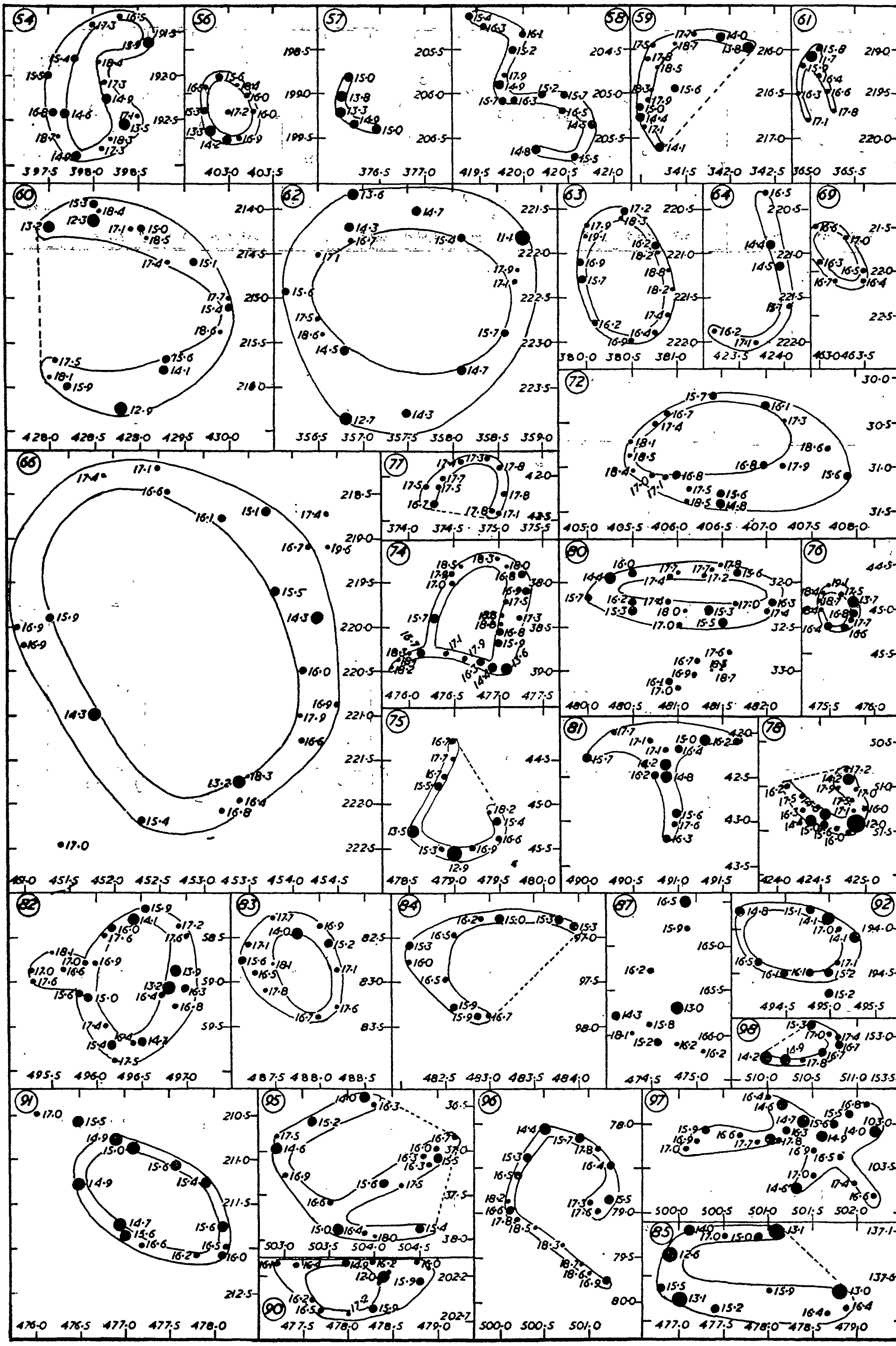

Fig. 2a

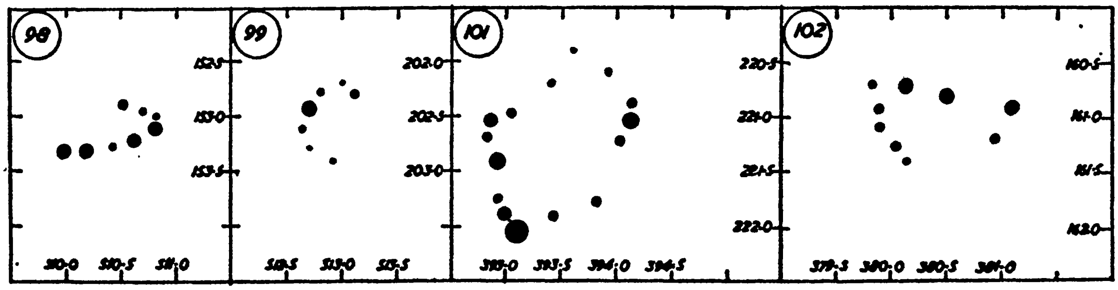

Fig. 3

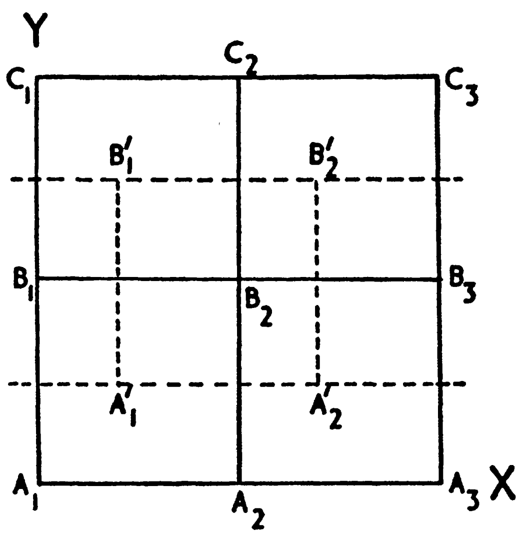

FIG 5a

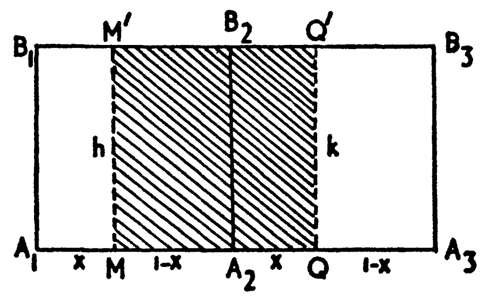

FIG 5b

Figs. 1, 2, 3. Unusual groupings in the Eta Carinae field, with rectangular coordinates in mm.

Figs. 1a, 2a. Same as Figs. 1, 2, with magnitudes and assumed grouping area boundaries indicated.

Fig. 4. Positions of the groupings and the Eta Carinae nebula, in rectangular (X, Y mm) and equatorial (α, δ 1875.0) coordinates.

Fig. 5. Foursome of squares in displaceable grid.

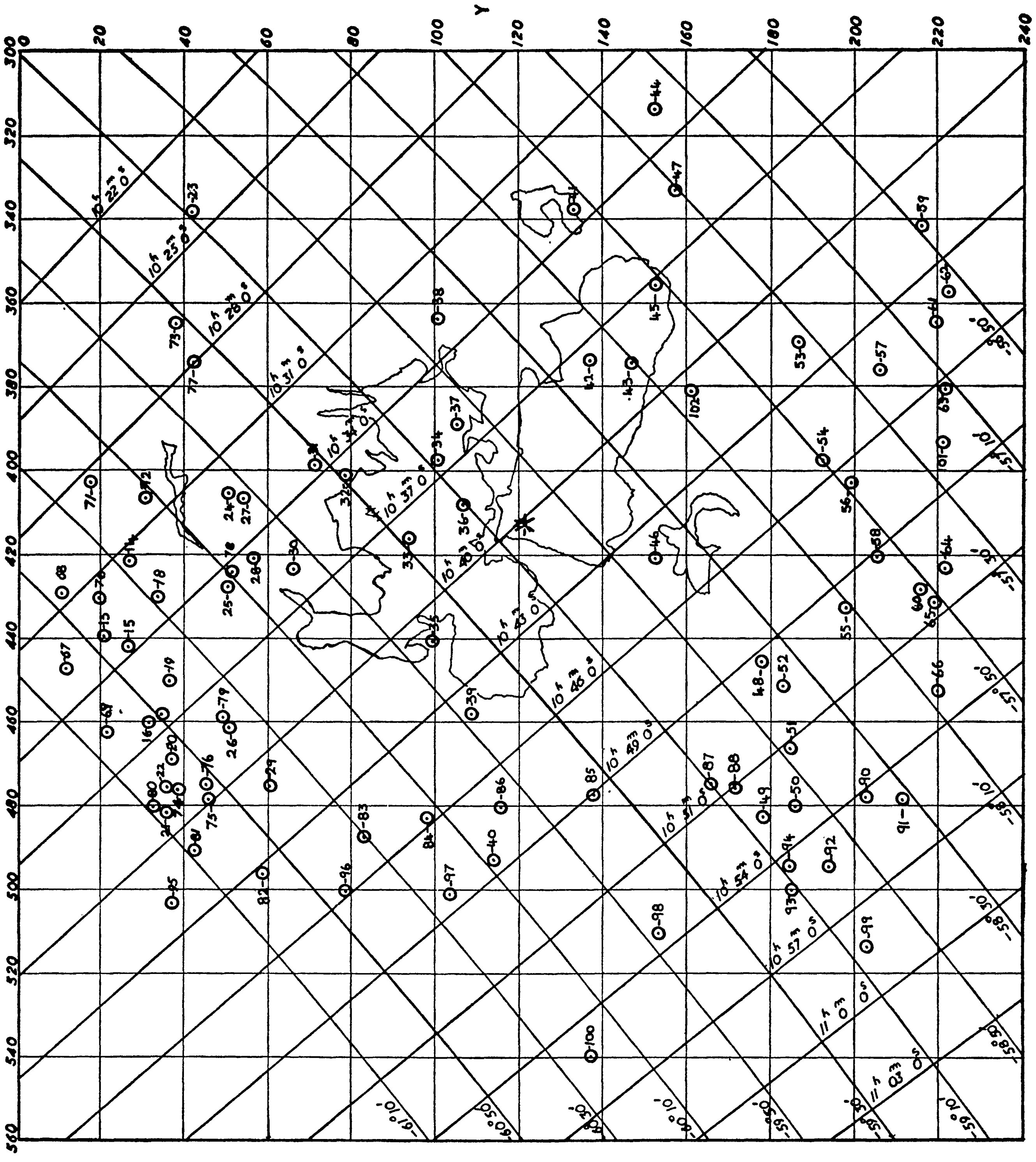

Fig. 4

Table 2

Astrometric Reference Stars

No.	CPD	mag.	α, 1875.0	δ, 1875.0	ξ''	η''	X mm	Y mm
1	—58°2380	7.1	$10^h31^m50^s$	—58°32′.5	—5247	—2142	353.0	101.1
3	—57°3909	7.4	10 47 21	—57 35 .3	+2149	—5666	399.8	211.2
4	—58°2834	5.6	10 48 24	—58 11 .2	+2566	—3503	426.0	192.0
5	—59°2860	7.6	10 51 10	—59 47 .1	+3703	+2284	494.5	139.1
6	—60°2203	6.4	10 38 27	—60 30 .9	—2015	+4872	456.7	55.3

The conversion can be achieved also graphically with the help of Fig. 4, on which also the positions of the groupings, of Eta Carinae, and of its nebula are shown. A glance at the figure reveals what may be a very significant detail: the groupings occupy mainly a semi-circular region, with Eta Carinae at the centre (on the figure above, below and to the left of the star). The radius of the semi-circle is about 1°30′ or 65 parsecs at the distance of the nebula, close to the size of supernova remnants or the final stages of expanding hydrogen rings in which star formation by way of dust nucleation has been suggested (*Refs*. 4, 5).

3. *Random Probabilities and Expectations*

The definition of what may appear an "unusual" grouping contains several attributes, none of which can be described precisely. The notion contains therefore a certain degree of vagueness which can be removed only by schematization. By cutting out some of the attributes (such as unusual brightness) and limiting the criteria to others which can be described mathematically (such as the areal density), probabilities of random occurrence can be calculated which, as far as omission of other criteria is concerned, are upper limits and, therefore, can be applied safely in judging the reality or randomness of the groupings.

On the other hand, with the sole criterion of areal density, the size, shape, and arbitrary position of the area in question introduce degrees of freedom which, though not changing the probability of a single grouping, increase its random expectation to be found on a plate in a ratio that may be considerably larger than the ratio of the area of the plate to that of the grouping. This expectation ratio can be assessed but approximately, because of the indefiniteness of shape to be recognized subjectively as a grouping. In restricting the freedom to elliptical or oval contours, the expectation ratios will be underestimated and can be calculated approximately, to an uncertainty factor of the order of unity, as shown below.

We start first with the simplest case of a fixed *prescribed* area s in a field (plate) of area S in which n points (stars) are distributed at random. The area may be one chosen individually in advance, without regard to its actual stellar content, or it could be one of a prescribed number N of squares of a reseau into which the plate is subdivided (*Refs.* 6, 7). The average density over s is

$$\rho = ns/S = pn, \tag{5}$$

where the probability for one object to fall on s is

$$p = s/S = 1/N, \tag{6}$$

and

$$N = S/s \tag{7}$$

for the reseau case.

The probability of having m points in s is exactly given by the appropriate $(m + 1)$th term of the binomial expansion

$$[p + (1 - p)]^n$$

and is

$$P_m = C_n^m \, p^m \, (1 - p)^{n-m} \tag{8}$$

where the coefficient is determined through the appropriate factorials,

$$C_n^m = n!/m! \, (n - m)! \tag{9}$$

The expected frequency of occurrence of m among fixed equal areas s (squares in the particular case of reseau), or the expectation of m is then

$$E_m = PN = PS/s, \tag{10}$$

the alternatives to be used according to the specific circumstances of the case (reseau, or not).

When n is large, and N also large or p small, the Poisson approximation can be used, instead of the exact formula (8); to first order terms the approximation is

$$P_m' = \{1 + (m/n) \, [1 - (m - 1)/2\rho]\} \, \rho^m \exp(-\rho)/m! \tag{11}$$

For applicability, the multiply bracketed factor must be close to unity and lie, say, between 1.20 and 0.80. The tolerance is quite high even for relatively small numbers, as can be seen from the following example for $n = 20$, $N = 10$, $\rho = 2$:

m	=	0	1	2	3	4	5	6	7	8
factor	=	1.00	1.05	1.075	1.075	1.05	1.00	0.925	0.825	0.70

Thus here Poisson's formula with the correction factor works well up to $m = 7$ or to the 3.5-fold of average density. For higher values of m from 8 to 20 it fails but the probabilities are very small in these cases and their exact values are of little practical significance. Usually Poisson's formula is taken without the correction factor, as for $m/n \to 0$.

The chain groupings as considered here can all be reduced to the particular case of two areas: one a void with $m = 0$ over an area $s - s_r$, the other containing all the n stars in the chain area s_r. Setting

$$p = (s - s_r)/s, \; (1 - p) = s_r/s, \tag{12}$$

the probability of the chain in fixed position is now given by the exact formula (8) as

$$P_0 = (1 - p)^n = (s_r/s)^n, \tag{13}$$

valid for $n_r = n$.

When $n_r < n$, the same formulae apply to a more restricted area, consisting of chain only plus the enclosed void,

$$s' = s_r + s_i, \tag{14}$$

to be used instead of s, with n_r substituted for n.

These probability formulae apply without restriction, depending only on the areas s_r and s of the configuration. With the freedom in displacement and shape, not restricted to a fixed reseau or grid, the expectation as compared to (10) will be increased by an amplification factor F, so that the expected number of voids on an area s (or $s_r + s_i$, according to the case) will be given by

$$E = E_o = FP_oS/s. \tag{15}$$

Consider a rectangular displaceable grid for ρ sufficiently large to disregard the overlapping of the voids (exp ρ large) at a fixed position of the grid. $F = F_1$, $P_o = (1—p)^n$, $E = E_1$ correspond to a total population $n_1 = n$ of the plate, so that

$$E_1 = F_1\ (1 - p)^n\ S/s. \tag{a}$$

Add now a random population t, so that, by virtue of equation (13), the number of voids will be changed by a factor of $(1 - p)^t$ and become

$$E_2 = F_1\ (1 - p)^{n+t}\ S/s. \tag{b}$$

On the other hand, when F_2 denotes the amplification factor for the total number $n + t$, equation (15) would require

$$E_2 = F_2\ (1—p)^{n+t}\ S/s. \tag{c}$$

From comparing (c) with (b) it follows that $F_2 = F_1 = F =$ const.

Thus, when overlappings are rare, the amplification factor is constant, independent of the population of the plate.

With the method of identification of the groupings, individual groupings or voids are listed independent of size; two or more adjacent voids are therefore entered as one individual. Hence, when ρ is small, and the probability of a void, exp $(—\rho)$ large, there are overlappings causing mergers and a decrease of the number of identified areas. In such a case the amplification factor will be smaller than its upper limit F considered above. By using F in all cases, the random expectation of voids as of equation (15) will be somewhat exaggerated; this will help to keep the estimates on the safe side.

4. *Amplification Factor in a Displaceable Rectangular Grid*

Consider a rectangular grid (reseau) of squares, superposed on a field of random points and displaceable parallel to its X and Y axes. When, in an initial fixed position, the expected number of voids is given by (10) with $P_m = P_o$ according to (13), further displacement may reveal new voids between the populated squares of the initial grid.

Let (Fig. 5a) A_1 C_1 C_3 A_3 be a foursome of adjacent squares of the initial fixed grid. In parallel displacement, the initial square $A_1B_1B_2A_2$ may be shifted into a new position, $A_1'B_1'B_2'A_2'$. If there was a void ($m = 0$) among the initial foursome, a void in the displaced position will overlap with the initial void and form one, larger void without increasing the number of individual voids in a list such as ours. If there was no initial void, one in the new position may occur by chance, adding thus to the amplification factor. Any void occurring in the displaced position will exclude new individual voids inside the foursome, by way of overlapping as before. The problem is thus to find, by successive movements of displacement, the probability of new voids on the condition that no voids from previous positions of the grid are present inside the boundaries of the foursome. It is sufficient to confine ourselves to the displacement of one single corner square, $A_1B_1B_2A_2$, into all possible positions inside the foursome; this is covered by displacing the point A_1 over all possible positions inside the corner square, and is equivalent to moving the entire grid within the limits of one side of the square, A_1A_2 and A_1B_1, in the two coordinates. It is easy to see that displacements larger than one length of the square do not introduce new combinations—everything is exactly repeated.

Thus, when at least one of the squares of the basic foursome (Fig. 5a) is a void, displacements do not add new individual voids and are irrelevant.

When one of the four basic squares (Fig. 5a) is a void, displacements can put a reseau square over a void somewhere in an intermediate position. As soon as one void is established, further displacements do not add new individual voids. New voids are to be looked for only when none of the previous positions of the reseau showed a void.

Consider first displacements in the abscissae between the two lower squares of the foursome, containing h and k (non-zero) points each (Fig. 5b) distributed at random. A square MM′Q′Q, displaced by a length $A_1M = x$ (when $A_1A_2 = 1$) has a fraction $p_1 = 1 - x$ in common with the left-hand basic square and a fraction $p_2 = x$ with the right-hand basic square. The probability of a void in the displaced square, requiring coincidence of voids in the two overlapping fractions, is then, according to equation (13),

$$P_x = x^h\ (1-x)^k. \tag{16}$$

This attains a maximum at

$$x_m = h/(h+k), \tag{17}$$

$$P_m = h^h\ k^k/(h+k)^{h+k}. \tag{18}$$

We assume now that the foursome is part of a large area so that the Poisson approximation as of equation (11) without correction factor applies to the frequency of the h and k numbers (excluding zero values). The probability of an intermediate void in optimum (maximum) position of the displaced square is than obtained by double integration (summation) over integer h and k values from 1 to ∞ (excluding the zeros),

$$P_i = \exp\ (-2\rho)\ \Sigma\Sigma\ P_m\ \rho^{h+k}/h\,!k\,!. \tag{19}$$

Calculations were made according to (19) for $\rho = 5$, $\exp\ (-\rho) = 0.00674$ (Poisson probability of voids) which is small enough to disregard overlapping of the voids. At this value of average density, $P_i = 214.9 \exp\ (-2\rho)$ (*see* Appendix) or

$$P_i = 1.449\ (\exp{-\rho}) = 1.449\ P_0 \tag{20}$$

was found. The coefficient $f' = 1.449$ is thus the partial amplification factor as due to optimum displacement along the bottom of the foursome (Fig. 5b). The lowest h, k values contribute most to P_i: 16.1% derives from $h, k \leqslant 2$;

37.9% from $\leqslant 3$; 60.3% from $\leqslant 4$; 77.2% from $\leqslant 5$.

When a void does not occur at optimum displacement, a new void may be found at an intermediate position but with a much lower probability due to "blocking" by the non-zero density at the optimum. This second probability is to be calculated in the same way as P_i but for the displacement between one of the basic squares and that in optimum position, and so on. These additional probabilities decrease rapidly in a converging series; from approximate estimates (sample cases) it was found that the total probability is only increased by one-fifteenth of P_i as due to intermediate chances. Instead of equation (20) we have thus, for the probability of voids due to displacement A_1A_2 between two basic non-zero squares,

$$P_1 = 1.55\ P_0 \text{ or } f_1 = 1.55. \tag{21}$$

Four such independent displacements of a square can be visualized in a foursome (Fig 5) of non-zero squares and along four strips $A_1A_2C_2C_1$, $A_1A_3B_3B_1$, $B_1B_3C_3C_1$, $A_2A_3C_3C_2$. When none of these displacements yields a void, a further chance is provided by intermediate displacements such as A_1' B_1' B_2' A_2' (Fig. 5a) displaced in the X-direction. For a middle band (along B_1B_3) the probability can again be assumed equal to P_1 or f_1 (a slight overestimate because now its top and bottom boundary squares are non-zeros). Bands displaced from the middle again yield rapidly decreasing probabilities, so that, by adding (approximately) one-fifteenth to f, all possible horizontal displacements add up to a probability of

$$P_2 = 1.65\ P_0 \text{ or } f_2 = 1.65. \tag{22}$$

The family of intermediate horizontal displacements covers all possible positions of the grid (if it is retained parallel to itself) and no new voids can be produced by intermediate vertical displacements.

Hence the amplification factor for the frequency of voids in a uniform displaceable grid of equal squares, remaining parallel to itself, consists of the following components in a foursome of adjacent squares:

the four basic squares yield $4f_0$	=	4.00
the four displacements between the basic squares yield $4f_1$	=	6.20
all remaining intermediate displacements yield f_2	=	1.65
The total over four squares is		11.85

or

$$F = 11.85/4 = 2.96$$

per square, to be used with equation (15).

This factor is based on calculations for $\rho = 5$ and, because of overlapping and approximate calculational procedures, may be too large by a few per cent. Otherwise, as shown above, it will not depend on the average density itself, applying thus to all values of ρ (if large enough to eliminate overlapping).

It may be added that the boundaries of a void are subject to a statistical uncertainty; in a Poisson distribution the 50% uncertainty limit of its area is $\Delta\ S/S = \pm\ 0.69/\rho$ where $0.69 = \ln 2$.

5. *Random Expectations of Chains*

The chains—mostly rings—registered in the Eta Carinae region, though not squares, are bounded by smooth elliptical or oval contours which can be considered a geometric restriction of the same kind as that of a square grid. There is some freedom in the axial ratio and direction of elongation. Considering all the circumstances, we may assume for the purely geometrical amplification factor (as distinct from restrictions here disregarded, imposed by the excessive brightness, possibly spectra and colours of the stars which could strongly counteract the factor) a round value of

$$F = 3 \pm 0.5.$$

With the area on the plate studied with the iris diaphragm photometer equal to $S = 30{,}000$ mm² (*cf.* Figure 4), equation (15) leads to the following expression for the expected number of groupings of given *or smaller* probability:

$$E = 90{,}000\ P_o/s, \tag{23}$$

with $s_r + s_i$ instead of s (mm²) when $n_r < n$. We note that P_o is a cumulative probability at the same time—there cannot be a number less than zero (or, also, $n_r > n$ is not possible), (For other small discrete values of m_i, e.g. $m_i = 2$, the cumulative probability is $P_2 + P_1 + P_o$ but, because of the rapid decrease of the three consecutive terms when n is not an insignificant number, the cumulative sum differs very little from its first term, P_2). The expectations—cumulative for all practical purposes—for the individual groupings, calculated according to (23), are given in the 13th column of Table 1. The corresponding probabilities (P_o) are by 4 — 6 orders of magnitude smaller and can be obtained by multiplying the E-values by a factor of $1.11 \times 10^{-5}\ s$.

6. *Statistical Analysis*

Table 3 summarizes the recorded distribution of the random expectations, E, of Table 1.

In the second column, ΔE is the random expectation of occurrence of a grouping on the plate within the stated limits of E, in the 3rd column ν is the number listed in Table 1; the 4th column gives the ratio, the 5th the difference which can be called the probable real number as based on geometry criteria alone, and the 6th contains the average number of stars in a grouping. Out of a total of 69 groupings, 42 as the sum total of the fifth column appear to be real "cosmogonic" groupings, mostly closed or semi-closed chains. They are certainly not produced by absorption through interposed globules. The six globules listed are all darker than the surrounding background as shown by the wedge readings (column 9 of Table 1): —5.7, —7.1, —0.6, —0.2, —1.4, —1.3, average—2.7, while the total average for 74 objects is +0.20 ±0.12 (p.e.), and for 67 objects, upon exclusion of the globules and a cluster, it is +0.40 ±0.13, indicating a mild brightening inside the rings.

Table 4 lists the average magnitude differences of the stars relative to the background (m_b), for 68 objects—67 chain groupings and one cluster—arranged in groups of E.

Table 3

Frequency of Random Expectations

E limits	ΔE	Number listed ν	Ratio $\nu/\Delta E$	Real number $\nu—\Delta E$	Average population n_r
0					
	0.0001	12	120000	12	25.7
10^{-4}					
	0.00090	4	4400	4	19.0
10^{-3}					
	0.009	7	780	7	14.6
10^{-2}					
	0.04	6	150	6	15.8
0.05					
	0.05	1	20	1.0	15.0
0.10					
	0.40	9	22	8.6	13.1
0.50					
	0.50	2	4	1.5	15.5
1.0					
	1.0	3	3	2.0	13.0
2.0					
	2.0	2	1.0	0.0	12.0
4.0					
	6.0	4	0.7	(0)	11.2
10					
	40	4	0.1	(0)	10.5
50					
	50	2	0.04	(0)	6.5
100					
	33,000	13	0.0004	(0)	9.2
33000					

Table 4

Average Magnitude Differences

(*see* Tables 1 and 3)

E	Number	$m_o—m_b$	$m_r—m_b$
<0.05	28	—3.05	—1.27
0.05—1.9	15	—3.51	—1.77
2.0—99	12	—3.41	—2.09
≥100	13	—3.36	—2.07

The differences are larger for the three groups with large E, indicating perhaps a subconscious emphasis on brightness in picking out groupings of less conspicuous geometry.

In a typical stellar distribution at $b = 0°$ and around magnitude 19.0 (*Ref.* 3), the median magnitude exceeds the limiting magnitude by about 1.0 mag as shown in Table 5.

Table 5

Limiting mag.	20.0	19.5	19.0	18.5	18.0
Median mag. (50% number)	18.92	18.50	18.03	17.53	17.09
Median-Limiting	—1.08	—1.00	—0.97	—0.97	—0.91

In a list that is incomplete near the limit (as all first-hand observational lists are bound to be) the median magnitude may be further shifted upwards by 0.5 mag and may stay about 1.5 mag brighter than the limit. The median magnitude of our groupings is about 3 mag above the limit, suggesting again excessive brightness of their members as an additional criterion of non-randomness. In a future more detailed research this circumstance must be given special attention with photometric measurements extending over the surrounding field and not restricted to the members of the grouping alone.

The probability for a listed grouping to be real depends on the ratio as given in the 4th column of Table 3. Practically all those with $E < 0.50$ must be considered as real, those with $E = 0.5$ to 2.0 are probably real, and many of those with larger E may be real, too, such as No. 47 containing exceptionally bright stars although its geometrical random expectation is as high as 7800.

7. *Review of Other Work and Discussion*

The notion of star chains has imposed itself on the imagination already in antiquity when the naked-eye stars were arranged in fanciful images of the constellations. It has persisted in our time, despite the difficulty of understanding how stars, despite their proper motions, could keep their regular ranks over the ages.

A complete survey of the northern sky down to magnitude 12.5 in this respect was made by Oberguggenberger (*Ref.* 8), restricting the groupings to nearly equidistant members of nearly equal brightness, aligned along a straight or slightly curved line. With these, cosmogonically incomprehensible, restrictions a list of about 500 items was constructed, most of which consisted of four stars only; as shown by Holmberg (*Ref.* 9), these groupings could be explained entirely as due to chance; and, if this were not so, "the existence of such chains would introduce further *undesirable* (*italics Ö.*) complications as regards our conception of the constituents of the Milky Way system". Of course, whether desirable or not, whether we like them or not, complications if based on fact have to be accepted. Groupings of four individuals only, unless very bright or very close together, can be easily produced by chance, and Holmberg's result in the present case was almost a foregone conclusion.

Bourgeois and Hunaerts (*Ref.* 10) subjected a choice sample of ten chains, recommended by Oberguggenberger as typical of his list, to a spectral and photometric analysis, with deduced absolute magnitudes and distances. Except for one chain, the distances of the individual members in each case are so widely different that there cannot be any question of their physical or genetic relationship. With an upper limit of length of 1—1.5 degrees of a chain, the dispersion in depth is 10—50 times the projected length. The only chain (F.A.150) whose members are at nearly "equal" distances (145, 105, 90, and 150 parsecs, respectively) may also be just a coincidence. This furnishes additional evidence that 0's chains are but fortuitous combinations.

The production of chains in experimental supposedly random populations (impacts of drops falling on paper, and photographed projection of three-dimensional clouds of non-soluble aniline particles suspended in a salt solution of equal density) has been investigated by Meurers (*Refs.* 11, 12). He was chiefly concerned with preferential directions of alignment which, in particular, are affected by the motion of the cloud, showing preference at right angles to the direction of motion. The latter phenomenon apparently shows that, contrary to Meurers' opinion, his experimental populations of points are not purely random arrangements but are influenced by the physical and mechanical conditions of the experiment. Surface tension of the particles of different size, and especially vortices of microturbulence in the liquid and the air, may have produced small-range interactions and groupings. Curiously enough, the artificial fields projected from suspended aniline clouds (*Ref.* 11, Fig. 8), or by falling droplets (*Ref.* 12, Figs. 6 and 7), abound in ring-shaped chains and voids of no less prominency than those marked by us in the Eta Carinae region. Meurers states (*Ref.* 12, p. 19, translation from German): "Those fluctuations of density in sparsely populated fields of points or stars are found also in dense fields, though in a different form, and lead, when the density is sufficiently high, to the well known circular voids in star fields, which are equally plentiful in artificial fields of points and in real star fields". In this statement, a theoretical inconsistency is obvious; it is submitted that increasing density of the points favours the chance occurrence of the lacunae, and of the very special type of circular voids. Now, if at a given density there is a certain number of gaps, by sprinkling over an additional random population many gaps will be filled, and the more so the greater the added density. Meurers' experiments seem to have shown the opposite which would indicate that the microscopic distribution of the points in his experiments was not at random. Besides, a glance at his experimental fields (*Ref.* 11, Fig. 8, and *Ref.* 12, Figs. 6 and 7) reveals large-scale variations in density, irreconcilable with randomness. In this respect probability calculus is the ultimate criterion of randomness, and this yields for the gaps in his reproduced denser fields probabilities of the order of 10^{-9} and less. Apparently, the physical interactions and vorticity in his experiments were thus not less efficient in producing the specific deviations from randomness than the alleged cosmogonic factors which have led to the ring-shaped star chains around Eta Carinae.

It seems that physical experiments purported to lead to randomness are always suspect, and that theory is the ultimate criterion. Unfortunately, because of the many degrees of freedom and the indefiniteness of the notion of a chain, precise theory cannot be produced and to the uninitiated there may seem to remain a margin of doubt. "Experimental theory"—a Monte Carlo method of constructing a field of points with the aid of coordinates read from a succession of random numbers (ten digits from 0 to 9 in an infinite random succession, combined into groups of eight, the first four for the X, the next for the Y coordinate), without the interference of physical factors, could be the answer.

A remarkable straightforward observational approach to the physical and cosmogonic implications of star chains has been made by Fessenkoff and Rojkovsky (*Ref.* 13). Based on photographs obtained since 1950 with the then new Maksutoff telescope near Alma-Ata (formerly Vernyi) in Kasakhstan, they maintain to have pinpointed star chains in the making, stars of the order of solar mass and of nearly equal luminosity condensing from nebular filaments, mixtures of gas and dust, into equidistant alignments. The regularity of these star chains is considered an indication of recent origin, being not older than 500,000 years, as over longer intervals they inevitably would have become scattered away from the place of origin. These researches have been commented upon by Struve (*Ref.* 14) and Kourganoff (*Ref.* 15). The chains around Eta Carinae may be of a similar origin, and may be related to supernova explosions (*Refs.* 4, 5).

Closest to our present work comes a study by Martynoff (*Ref.* 16). He points out the omnipresence of star chains in the Milky Way, especially in some peculiar regions, as in the vicinity of the N. America Nebula. On plates down to limiting magnitude 17.5, the chains comprise 15-20 and more members from the 11th to the 15th magnitude. On an area of 6.9 square degrees, there are 23 chains containing more than 15 members, while the mathematical expectation (E in our notation) is only 0.017. Cosmogonic interpretations are also given.

Three remarkable star chains are pointed out by Miss Pismis (*Ref.* 17) in the field of the Rosetta Nebula (NGC 2237) in Monoceros, in which the cluster NGC 2244 is imbedded ($\alpha = 6^h27^m.0$, $\delta = +4°56'$, 1900). With 25 to 40 bright members each (and many fainter ones), these chains form concentric arcs with the nebula, similar to some nebular wisps. The colour-magnitude diagrams of the chains and the cluster appear to be identical except for the earliest spectral types which are absent in the chains. Cosmogonic implications seem to point toward star formation in concentric shells expelled from the nebula.

"Negative" star chains, projected on the background of the cluster Omega Centauri (*Ref.* 18, Plate XVII), are thin dark lanes undoubtedly due to interposed absorbing filaments. The spaces between three parallel dark lanes appear as extended star chains of 50-100 members or more. This reminds us of obscuration as another factor which can produce chains of a high statistical level of significance without implying a real grouping of their members.

Purely statistical criteria for the star chains must be supplemented by photometric observations. In such a manner, it is shown by Dibay (*Ref.* 19) that out of 14 investigated chains to NE of the North America Nebula (α = 21^h04^m, $\delta = +46°.0$, 1900), three with a high statistical level of significance show a close correlation of colour index with apparent magnitude seemingly corresponding to the Main Sequence; this supports the physical reality of these three chains. The remaining 11 chains show complete scatter in the colour magnitude diagram, as is the case also with a comparison field. These eleven chains thus may not be real, although a large and unusual proportion of giant or semigiant stars, together with a few field stars admixed could produce a similar scatter in a physically real chain.

The preceding review of former work is only meant to convey an idea of the different problems involved, without attempting an exhaustive enumeration of all the work done in this respect. Of the points that emerged, the most serious appears to be the purportedly random experiments by Meurers, which have yielded chains and round voids of a high statistical level of significance. However, while awaiting the results of specially planned Monte Carlo experiments, free from all physical factors, the validity (to a close order of magnitude) of our statistical treatment can be checked by similar experiments made in a somewhat different setting (*Ref.* 7). The probabilities of random configurations, groups of squares in contact along one side at least, were experimentally investigated and theoretical formulae given which turned out to be in good agreement with experiment. A number t (denoted m in the original work) of "marked" squares was distributed at random in a grid (reseau) of $N = 169$ squares (as on the Carte-du-Ciel maps) and the numbers $x_1, x_2, x_3 \ldots x_t$ of groups consisting of one, two, three, etc. individuals were counted; evidently

$$t = \Sigma\, ix_i \ (i \text{ from } 1 \text{ to } t). \tag{24}$$

Such grouping does not depend on the qualifications of the marked squares. Now assume that the marked squares are voids ($m_i = 0$). The Poisson approximation applies here closely (*N is large*) and, if the observed number of voids, t, is to be identified with the mathematical expectation (thus equating a variable quantity to its average), $t = E_m$, according to (11) and (10) with $m = 0$ we have for the equivalent density of points per square the expression

$$\rho = -\ln(t/n) = \ln(N/t). \tag{25}$$

For a group of i ($i = 1, 2, 3, \ldots$) adjacent squares, the density is

$$\rho_i = i\rho, \tag{26}$$

whence, according to equations (15), (11), (25) and (26), the cumulative number of groups or voids each consisting of i squares or more can be represented as (considering that $S/s = N/i$)

$$E_i = (N/i)f_i\ (t/N)^i \tag{27}$$

where f_i is the empirical amplification factor due to freedom of choice in the arrangement of the squares. This is expected to be related to the factor F of equation (15) with a difference: F refers to the limiting case of considerable

Table 6

Indirect Values of the Group Amplification Factor (f_i) experimentally determined (for $t < 5$ theoretically interpolated) (*Ref.* 7) ($N = 169$)
(n_o is the cumulative number of experimental groups)

t =	2	3		4			5	
ρ =	4.44	4.03		3.74			3.52	
i =	2	2	3	2	3	4	2	3
E_i =	0.022	0.065	0.008	0.133	0.00294	0.000035	0.234	0.004
f_i =	1.9	2.4	2.5	2.81	3.95	2.65	3.16	2.7
n_o =	...	...	...	...	...	...	61	1

t =	10		15			20			
ρ =	2.83		2.42			2.13			
i =	2	3	2	3	4	2	3	4	5
E_i =	0.94	0.08	1.84	0.35	0.09	3.12	0.59	0.12	0.03
f_i =	3.24	6.8	2.77	8.9	35	2.64	6.3	14	380
n_o =	120	10	162	31	8	200	38	8	2

t =	25					30				
ρ =	1.91					1.74				
i =	2	3	4	5	6	2	3	4	5	6
E_i =	4.27	1.17	0.44	0.19	0.02	5.97	2.07	0.65	0.25	0.10
f_i =	2.32	6.4	22	79	120	2.76	6.6	16	42	112
n_o =	205	56	21	9	1	239	83	26	10	4

t =	35					40				
ρ =	1.58					1.44				
i =	2	3	4	5	6	2	3	4	5	6
E_i =	7.24	2.99	1.15	0.43	0.12	8.57	4.19	2.00	1.12	0.65
f_i =	2.00	6.0	15	33	54	1.81	5.6	15	45	130
n_o =	232	96	37	14	4	274	134	64	36	21

ρ-values, low expectations and little overlapping, while f_i is derived from experiments with considerable t-values, for purely practical reasons ($t > 1$ in any case!) which requires low density and leads to "tunnelling" of the empty squares forming long-drawn fancy chains. For these low values of ρ therefore the number of groups increases in a kind of breakthrough and f_i reaches large values. For our concepts we should expect $f_i \rightarrow F$ when ρ increases and i decreases. This must be kept in mind when considering the "experimental" values of f_i in Table 6, as calculated according to equation (27).

The curious increase of the f_i-values with i, the number of elements, is characteristic of the "tunnelling" at these low population densities, with $\rho = 1.5$ to 2.5 per square.

The average density per area of the Eta Carinae groupings, $\rho = n_r$

(Table 3), is very much higher, the groupings picked out are more compact and the areas restricted in their relative dimensions. The cases of $i = 2$ and 3 of the higher densities (first row of Table 6) are most appropriate for the comparison. A value of $F = f_i \sim 3$ suggests itself indeed for the amplification factor as actually used. Thus, despite the contrary interpretation by Meurers (*Ref.* 12), we feel that the non-randomness or the reality of most of the groupings picked out in the Eta Carinae region is strongly indicated.

It may be added that the search of groupings was by no means exhaustive, and those listed are comprised within a definite range of sizes, the upper limit being determined by the field of the microscope used in the search, the lower limit depending on the star density which was about 14 stars per square millimetre or 39,000 per square degree. The distribution of the equivalent diameters of the areas (diameter of circle with an area equal to s) is given in Table 7. The median diameter is about 1′.4.

Table 7

Distribution of the Diameters (D, minutes of arc) of the Areas in Table 1

D	0.6—0.8	0.8—1.0	1.0—1.2	1.2—1.5	1.5—2.0	2.0—3.0	3.0—4.5	All
Number	9	8	10	11	19	9	4	70

References

(1) E M. Lindsay, *Irish Astron. J.*, 1, p. 141, 1950.
(2) E. M. Lindsay, *Irish Astron. J.*, 2, p. 140, 1953.
(3) F. H. Seares, P. J. van Rhijn, Mary C. Joyner, and Myrtle L. Richmond, *Astrophys. J.*, 62, p. 320, 1925; *Mount Wilson Contribution* No. 301.
(4) E. J. Öpik, *Irish Astron. J.*, 2, p. 219, 1953; *Armagh Obs. Leaflet* No. 22.
(5) E. J. Öpik, *Mém. Soc. R. Sc. Liège*, 8vo, 15, p. 634, 1955; *Armagh Obs. Leaflet* No. 34.
(6) E. J. Öpik and M. Lukk, *Tartu Obs. Public.*, 26, No. 2, 176 pp., 1924.
(7) E. Öpik, *Tartu Obs. Public.*, 27, No. 7, 28 pp., 1934.
(8) V. Oberguggenberger, *Zeits. f. Astrophysik*, 16, p. 323, 1938.
(9) Erik Holmberg, *Zeits. f. Astrophysik*, 18, p. 132, 1939.
(10) P. Bourgeois and J. Hunaerts, *Bull. Astron. Uccle*, 3, p 157, 1942.
(12) J. Meurers, *Bonn Veröff.* No. 37, 1951.
(12) J. Meurers, *Bonn Veröff*, No. 45, 1957.
(13) V. G. Fessenkoff and D. A. Rojkovsky, *Russian Astron. J.*, 29, pp. 382 & 397, 1952; 30, p. 3, 1953.
(14) O. Struve, *Sky and Tel.*, 13, p. 181, 1954.
(15) V. Kourganoff, *Contrib. Lab. Astr. Lille*, No. 2, 1954.
(16) D. Martynoff, *Astron. Circ. Ac. Sc. USSR*, No. 148, p. 14, 1954.
(17) Paris Pismis, *Bull. Tonantzintla & Tacubaya*, No. 13, p. 23, 1955.
(18) A. P. FitzGerald, *Irish Astron. J.*, 3, p. 204, 1955; *Armagh Obs. Leaflet* No. 38.
(19) E. A. Dibay, *Astron. Circ. Ac. Sc. USSR*, No. 186, p. 15, 1957.

Appendix

The Probability Integral of Equation (19)

(Calculations by Mrs. Alide Öpik)

(1) Auxiliary Table

n	1	2	3	4	5	6	7	8	9	10
$\log n^n$	0.0000	0.6020	1.4313	2.4084	3.4950	4.6692	5.9157	7.2248	8.5878	10.0000
$\log n!$	0.0000	0.3010	0.7782	1.3802	2.0792	2.8573	3.7024	4.6055	5.5598	6.5598
$\log (n^n/n!)$	0.0000	0.3010	0.6531	1.0282	1.4158	1.8119	2.2133	2.6193	3.0280	3.4402

n	11	12	13	14	15	16	17	18	19	20
$\log n^n$	11.4554	12.9504	14.4807	16.0454	17.6415	19.2656	20.9168	22.5954	24.2972	26.0200
$\log n!$	7.6012	8.6803	9.7943	10.9404	12.1165	13.3206	14.5511	15.8063	17.0851	18.3861
$\log (n^n/n!)$	3.8542	4.2701	4.6864	5.1050	5.5250	5.9450	6.3657	6.7891	7.2121	7.6339

(2) Table of $P_m\ \rho^{h+k}/h!k!$ for $\rho = 5$

$h =$ / k	1	2	3	4	5	6	7	8	9	10	sum >10
1	6.252	9.262	10.980	10.670	8.722	6.155	3.806	2.101	1.042	0.472	0.350
2	9.262	9.763	9.000	7.145	4.944	3.021	1.650	0.813	0.365	0.151	0.105
3	10.980	9.000	6.776	4.556	2.730	1.473	0.718	0.321	0.131	0.050	0.030
4	10.670	7.145	4.556	3.339	1.404	0.676	0.299	0.122	0.046	0.016	0.008
5	8.722	4.944	2.730	1.404	0.663	0.289	0.117	0.044	0.015	0.005	0.002
6	6.155	3.021	1.473	0.676	0.289	0.115	0.043	0.015	0.005	0.001	0
7	3.806	1.650	0.718	0.299	0.117	0.043	0.015	0.005	0.001	0.000	0
8	2,101	0.813	0.321	0.122	0.044	0.015	0.005	0.001	0.000	0	0
9	1.042	0.365	0.131	0.046	0.015	0.005	0.001	0.000	0	0	0
10	0.472	0.151	0.050	0.016	0.005	0.001	0.000	0	0	0	0
11—∞	0.350	0.105	0.030	0.008	0.002	0	0	0	0	0	0
1—∞	59.812	46.219	36.765	28.518	18.935	11.793	6.654	3.427	1.605	0.695	0.495

Total sum, extrapolated to infinity: 214.918.

Armagh Observatory,

November 14, 1968